Nanopatterning on Nonplanar and Fragile Substrates with Ice Resists

Nanopatterning on non-planar and fragile substrates with ice resists

*Anpan Han[1†], Aaron Kuan[2], Jene Golovchenko[1,2], and Daniel Branton[3]**

[1]Department of Physics, Harvard University, Cambridge, Massachusetts 02138, USA, [2]School of Engineering and Applied Sciences, Harvard University, Cambridge, Massachusetts 02138, [3]Department of Molecular and Cellular Biology, Harvard University, Cambridge, Massachusetts 02138

[†]Current address: Interdisciplinary Nanoscience Center and Department of Physics and Astronomy, University of Aarhus, 8000 Aarhus C, Denmark.

RECEIVED DATE:

RUNNING TITLE HEAD: Non-planar Nanopatterning with Ice Resists

*Corresponding author: Daniel Branton dbranton@harvard.edu

ABSTRACT

Electron beam (e-beam) lithography using polymer resists is an important technology that provides the spatial resolution needed for nanodevice fabrication. But it is often desirable to pattern non-planar structures on which polymeric resists cannot be reliably applied. Furthermore, fragile substrates such as free-standing nanotubes or thin films cannot tolerate the vigorous mechanical scrubbing procedures required to remove all residual traces of the polymer resist. Here we demonstrate several examples where e-beam lithography using an amorphous ice resist eliminates both of these difficulties and enables the fabrication of unique nanoscale device structures in a process we call ice lithography[1,2]. We demonstrate the fabrication of micro and nanostructures on the tip of atomic force microscope probes, micro cantilevers, transmission electron microscopy grids, and suspended single-walled carbon nanotubes. Our results show that by using amorphous water ice as an e-beam resist, a new generation of nanodevice structures can be fabricated on non-planar or fragile substrates.

KEYWORDS

non-planar, nanopatterning, e-beam lithography, ice lithography, resists

MANUSCRIPT TEXT

We consider first the fabrication of a rectangular metallic cap on the pyramidal tip of a standard atomic force microscope (AFM) cantilever (Fig. 1a). A cantilever was loaded onto a cryostage in a field emission scanning electron microscope (SEM) that had been modified for ice lithography[3]. The sample was cooled to <120 K on the SEM cryostage. Water vapor was then introduced into the SEM vacuum chamber from a nozzle mounted above the cryostage and deposited ballistically onto the cold sample. At temperatures <120 K, the water vapor condenses as an amorphous layer of ice that coats all accessible surfaces[1]. (Depending on the water vapor nozzle configuration and vacuum conditions during ice deposition, this deposition can be ballistic or totally conformal.) The focused e-beam of the SEM was then scanned in a rectangular pattern to remove the ice at the cantilever's tip and expose the underlying substrate[1]. Without breaking vacuum, the sample was subsequently transferred to a cold stage in an attached, pre-evacuated, metal deposition chamber where 1 nm of Ti and 20 nm of Au were sputter deposited onto the ice patterned surface. (All ice and metal thicknesses are stated normal to the plane of the horizontal cold stage.)

The cold sample was then removed from the vacuum and lift-off was performed by immersing it into room temperature isopropanol. Although isopropanol has the advantage of evaporating rapidly, we have successfully used other liquids, including distilled water[1]. As the ice melted, the deposited Ti/Au layer adhered only to what had been ice-free substrate areas.

The resultant metal-coated AFM tip shown in Figs. 1b and c is pyramidal with the four sides forming a very sharp apex. The lift-off is clean with no undesired metal flakes, and the roughly rectangular shape of the Ti\Au cap is clearly visible. While this sub-microscale rather

than nanoscale cap was fabricated to be clearly visible on an easily recognizable AFM cantilever, we have also written truly nanoscale features on other cantilevers and show some of these below.

Patterning on AFM tips has many applications. For example, a method of studying the binding forces between two biomolecules involves coating an AFM tip with gold and immobilizing biomolecules on the probe using sulfur chemistry. Patterning gold onto only the probe tip would allow precise control over the location, quantity, and geometry of immobilized biomolecules. Other applications of patterned AFM tips include tip enhanced Raman spectroscopy for chemical analysis and nano plasmonics[4], magnetic force microscopy, scanning single-electron transistor microscopy for studying mesoscopic systems[5], and other AFM related fields.

Patterning on the cantilever rather than the AFM tip is also of interest. For example, cantilevers with added metal structures have been used to study fundamental quantum mechanical systems such as Bose-Einstein condensates[6] and mesoscopic persistent currents[7]. But fabricating such cantilevers starting with planar blank wafers, as did Bleszynski-Jayich *et al.*[8], can be painstaking and time-consuming. Ice lithography made it possible for us to avoid many of the time-consuming steps by creating analogous metal structures on a commercially available silicon micro-cantilever (Fig. 2). For electrical insulation, a 100 nm thick silicon dioxide layer was first grown on the silicon cantilever by thermal oxidation. Ice lithography was then used to layer bonding pads for electrical connections and 500 nm wide, 300 μm long wires of 30 nm thick Au on 1 nm thick Ti. The resulting gold film was reflective, showed no discoloration, and the lift-off was very clean over the entire sample. Much narrower metal lines can also be patterned on AFM cantilevers (Fig. 2, inset); the narrowest metal lines we patterned onto AFM cantilevers were 15 nm wide.

In separate experiments, we measured the room temperature electrical properties of ice lithography-prepared Au and Pd wires that were 10 nm thick and 500 nm wide. The resistivities were respectively 150 and 500 nΩm, which is between 5 and 6 times higher than bulk values. This is typical for very thin films with high surface and grain boundary scattering[9,10]. In addition to low melting point metals we have also made nanostructures with tantalum, which has a very high melting point at 3017 °C. We can deposit almost any material with high purity by in-situ sputtering whereas methods such as gas-assisted focused electron and ion beam deposition are limited by the choice of materials and tend to incorporate contaminants that range between 20% to 90% of the total deposited material[11].

We also patterned the surface of fragile freestanding Si_3N_4 membranes supported on a Si wafer frame shaped like an electron microscope grid (Fig. 3). Silicon nitride membranes find important applications as platforms for plasmonic nanostructures[12,13] and nanopores[14] but are too fragile to withstand ultra-sonication, which is usually used with polymeric resists to assist lift-off. For example, in connection with a plasmonics research project we needed a thin silicon nitride membrane bearing metallic structures that were separated from each other by a nanogap. Because two triangular shapes with closely spaced apices lend themselves to forming such gaps, we fabricated an array of variously shaped triangular pairs (Fig. 3b, inset). By simply patterning the ice with triangular shapes separated from each other with the desired gap width, we created metallic structures with features less than 10 nm wide (Fig. 3a) and achieved gaps less than 7 nm wide (Fig. 3b). Note that the lift-offs were very clean with no undesired metal flakes. Characterization of these structures by transmission electron microscopy (TEM) and in-situ qualitative X-ray photoelectron spectroscopy showed no stray metallic material in the gaps fabricated between the structures.

Even the back side of the Si_3N_4 membranes, that are accessible at the bottom of the 200-μm deep pits etched through the Si wafer, were straightforward to pattern with ice lithography (Figs. 3c and d). It would not be possible to apply a controlled, homogeneous spin coated resist in such deep pits. The patterns shown in Fig. 3 were on 60 nm thick Si_3N_4, but we have also successfully patterned on membranes as thin as 20 nm.

Single-walled carbon nanotubes (SWCNT) are quasi one-dimensional nanostructures that have been studied extensively because of their superior physical properties and potential applications. But lithographically patterning freely suspended SWCNT using spin-coated resists is not possible because such freely suspended SWCNT are both non-planar and very fragile. We grew electrical insulating nanoparticles coaxially on freely suspended nanotubes or small bundles of nanotubes using ice lithography (Fig. 4). The carbon nanotubes were first grown over a 1 μm wide trench in a free standing silicon nitride membrane[2]. As previously described, ice-covered nanotubes can be imaged through the ice in the SEM using electron doses four orders of magnitude smaller than that required for actual patterning[2]. We then removed several 25 nm long regions of ice, each ice-free region separated from the next by 150 nm (Fig. 4a, inset). The white arrows show the locations where ice was removed. After writing and transfer to the metal deposition side chamber, 5Å of Ti was sputter deposited on the sample to form an adherent coating on the ice-free regions of the nanotubes.

After removal from the ice lithography SEM and immersion in isopropanol, the sample was dried by carbon dioxide critical point drying to avoid violent interfacial forces. Subsequently, the sample was transferred through air into an atomic layer deposition (ALD) chamber where 20 nm of Al_2O_3 was grown at 225°C on to the free standing nanotubes. ALD does not grow on pristine SWCNTs[2,15], but does of course grow on oxides. Upon exposure to

air, the patterned Ti on the nanotubes forms a surface oxide that initiates patterned ALD growth on the nanotube. As a result, Al_2O_3 nanoparticles were formed on the SWCNT. The overall geometry of these nanoparticles, including their location, was precisely determined by the ice lithography patterning and ALD processing parameters that deposited the Al_2O_3.

Our results demonstrate the utility of ice lithography for patterning and lift-off on non-planar and fragile substrates and show the adaptability of a simple water-ice resist in e-beam lithography. Since ice lithography can pattern silicon dioxide lines down to 5 nm wide[1] and metal wires down to less than 10 nm wide[3], it achieves as great or greater resolution than e-beam lithography using polymer resists. But because an ice resist is easily removed, leaving no residue following a dip in isopropanol or any other volatile solvent, ice lithography can be used to fabricate carbon nanotube field effect transistors and other fragile devices whose performance would be compromised by the residue of polymeric resists. Some polymeric resists can be deposited on non-planar surfaces[16], but their reliable removal, especially from fragile substrates, is problematic. Although the critical electron dose for water ice removal is roughly three orders of magnitude larger than that required for the typical exposure of a polymeric resist such as polymethyl methacrylate (PMMA)[1], the low sputter yield for water (0.03 H_2O molecules ejected per incident 5 keV electron[1]) will not be a serious concern in most situations where e-beam lithography is used for research or mask fabrication, rather than direct high volume commercial device production. Furthermore, the low sputter yield for water ice makes it possible to visualize and map the exact location of critical nanostructures through the ice layer without removing significant amounts of the overlying ice[2]. Such through-resist mapping can be very advantageous because the desirable properties of many nano-structures, such as carbon

nanotubes, are easily compromised by contamination or damage during unprotected direct exposure to the e-beam of an electron microscope[2,17].

Our demonstration that ice lithography enables the fabrication of nanostructures on non-planar and fragile substrates opens the possibility of research with nano-device configurations that have previously been difficult or impossible to obtain. These include devices with localized metal structures on CNT tips for high resolution magnetic force microscopy[18], improved and simplified production of tip enhanced Raman spectroscopy cantilevers[4], and metal enhanced fluorescence nanotubes[19]. In addition, ice lithography enables many other sensors and devices that are dependant on materials (such as graphene or even biological components) whose performance can be undesirably altered by e-beam exposure damage during fabrication, organic solvents during resist development, or by unwanted residues of polymeric resists.

Methods

All of the ice lithography steps and SEM imaging were performed in a modified field emission scanning and e-beam writing JEOL JSM-7001F SEM, as previously described[2,3]. The modifications of the SEM include a cryogenically insulated stage that could be cooled to <120 K with liquid nitrogen, liquid N_2 cooled baffles and cold fingers, and a second cold stage in a metal sputter-deposition chamber. The sputter-deposition chamber also served as a high-vacuum load lock that could be isolated from the JEOL main chamber by closing a gate valve.

ACKNOWLEDGEMENTS

Supported by grant R01HG003703 from the National Human Genome Research Institute, NIH to J.G. and D.B. The authors thank Dr. David Hoogerheide for assistance in TEM imaging and the Carlsberg Foundation for supporting A. H. with a post-doctoral grant.

REFERENCES

(1) King, G. M.; Schurmann, G.; Branton, D.; Golovchenko, J. A. *Nano Letters* **2005,** *5*, 1157-1160.

(2) Han, A.; Vlassarev, D.; Wang, J.; Golovchenko, J. A.; Branton, D. *Nano Lett.* **2010,** *10*, 5066-5059.

(3) Han, A.; Chervinsky, J.; Branton, D.; Golovchenko, J. A. *Review of Scientific Instruments* **2011,** *82*, 065110-065111 - 065110-065116.

(4) Yeo, B. S.; Stadler, J.; Schmid, T.; Zenobi, R.; Zhang, W. H. *Chemical Physics Letters* **2009,** *472*, 1-13.

(5) Martin, J.; Akerman, N.; Ulbricht, G.; Lohmann, T.; Smet, J. H.; Von Klitzing, K.; Yacoby, A. *Nature Physics* **2008,** *4*, 144-148.

(6) Treutlein, P.; Hunger, D.; Camerer, S.; Hansch, T. W.; Reichel, J. *Physical Review Letters* **2007,** *99*, 140403-140401 - 140403-140404.

(7) Bleszynski-Jayich, A. C.; Shanks, W. E.; Peaudecerf, B.; Ginossar, E.; von Oppen, F.; Glazman, L.; Harris, J. G. E. *Science* **2009,** *326*, 272-275.

(8) Bleszynski-Jayich, A. C.; Shanks, W. E.; Ilic, B. R.; Harris, J. G. E. *J. Vac. Sci. Technol. B* **2008,** *26*, 1412-1416.

(9) Brandli, G.; Olsen, J. L. *Materials Science and Engineering* **1969,** *4*, 61-83.

(10) Chopra, K. L.; Bobb, L. C. *Acta Metallurgica* **1963,** *12*, 807-811.

(11) Utke, I.; Hoffmann, P.; Melngailis, J. *Journal of Vacuum Science & Technology B* **2008,** *26*, 1197-1276.

(12) Koh, A. L.; Fernandez-Dominguez, A. I.; McComb, D. W.; Maier, S. A.; Yang, J. K. W. *Nano Letters* **2011,** *11*, 1323-1330.

(13) Schuller, J. A.; Barnard, E. S.; Cai, W.; Jun, Y. C.; White, J. S.; Brongersma, M. L. *Nature Materials* **2010,** *9*, 193-204.

(14) Li, J.; Stein, D.; McMullan, C.; Branton, D.; Aziz, M. J.; Golovchenko, J. A. *Nature* **2001,** *412*, 166-169.

(15) Farmer, D. B.; Gordon, R. G. *Nano Lett.* **2006,** *6*, 699-703.

(16) Parikh, D.; Craver, B.; Nounu, H. N.; Fong, F.-O.; Wolfe, J. C. *J. Microelectromechanical Systems* **2008,** *17*, 735-740.

(17) Cao, J.; Wang, Q.; Dai, H. *Nature Mater.* **2005,** *4*, 745-749.

(18) Deng, Z.; Yenilmez, E.; Leu, J.; Hoffman, J. E.; Straver, E. W. J.; Dai, H.; Moler, K. A. *App. Phys. Lett.* **2004,** *85*, 6263-6265.

(19) Hong, G.; Tabakman, S. M.; Welsher, K.; Wang, H.; Wang, X.; Dai, H. *J. Am. Chem. Soc.* **2010,** *132*, 15920-15923.

FIGURE LEGENDS

Figure 1. Ice lithography to cap an AFM Si_3N_4 tip with gold. **a**, Processes for ice lithography. Amorphous ice (cyan/white) is condensed on all accessible surfaces of a non-planar sample at <120 K. The e-beam is used to remove ice in the desired pattern, here a 600 X 600 nm rectangular pattern centered on the pyramidal AFM tip. 1 nm of Ti and 20 nm of Au (yellow) are deposited over the entire sample. After removing the sample from the vacuum, it is immersed in isopropanol at room temperature. The ice melts and only the metals deposited on the ice-free specimen surfaces remain. Since both the ice and metals are deposited under ballistic conditions, the cross-sectional view illustrates how the film thickness depends on the sample geometry. **b** and **c**, SEM images of commercial AFM probes whose tip had been capped with 1 nm thick Ti and 20 nm thick Au. The ice resist was 400 nm thick. A 100 pA, 15 keV e-beam dose of 3 C/cm^2 was used to pattern the rectangle on the AFM tip.

Figure 2. Ice lithography to wire a cantilever. **a,** Optical microscope and **b,** SEM images of a 125 μm long, 50 μm wide, 3 μm thick microcantilever onto which 0.5 μm wide, 300-μm long wires with bonding pads were formed by depositing 30 nm thick Au on 1 nm thick Ti. The ice resist was 160 nm thick and was patterned with a 3 nA, 10 keV e-beam dose of 1.5 C/cm^2. The inset shows a pattern of 50 nm wide, 5 nm thick Ti wires written on another cantilever using an 80 nm thick ice resist patterned with a 15 keV e-beam dose of 5 μC/cm.

Figure 3. TEM and SEM images of metal patterns on free-standing Si_3N_4 membranes. **a,** TEM images of three-bladed 5 nm thick Pd and **b**, TEM image of 5 nm thick Au on 1 nm thick Cr patterns on the planar top surface of a free-standing 60 nm thick Si_3N_4 membrane showing one of the gaps from an array (inset, SEM image) of similarly produced triangular

shapes . **c** and **d**, SEM images of 10 nm thick Ag on 1 nm thick Ti patterns near the edge of a 200μm deep pit on the bottom-facing surface of the 20 nm thick Si_3N_4 membrane. For **a** and **b,** 40 nm of ice was deposited and patterned with a 200 pA, 30 keV e-beam dose of 5 C/cm^2. For **c** and **d,** 160 nm ice was deposited and patterned with a 200 pA, 5 keV e-beam dose of 8 μC/cm.

Figure 4. Growing nanoparticles on SWCNTs. a, TEM of Al_2O_3 nanoparticles grown by ALD on a bundle of SWCNTs on which 5Å Ti had previously been deposited during ice lithography. White arrows indicate areas from which the ice had been removed by the e-beam; the purple bar shows the width of the ice-freed regions. The nanoparticles are sufficiently electron transparent that the nanotubes are clearly visible even where they are coaxially coated by the Al_2O_3. **Inset:** SEM image of patterned ice resist on the nanotubes before Ti deposition. **b,** Schematic of the experiment (not to scale). A 100 pA, 30 keV e-beam dose of 3 C/cm^2 was used to pattern a 60 nm layer of ice.

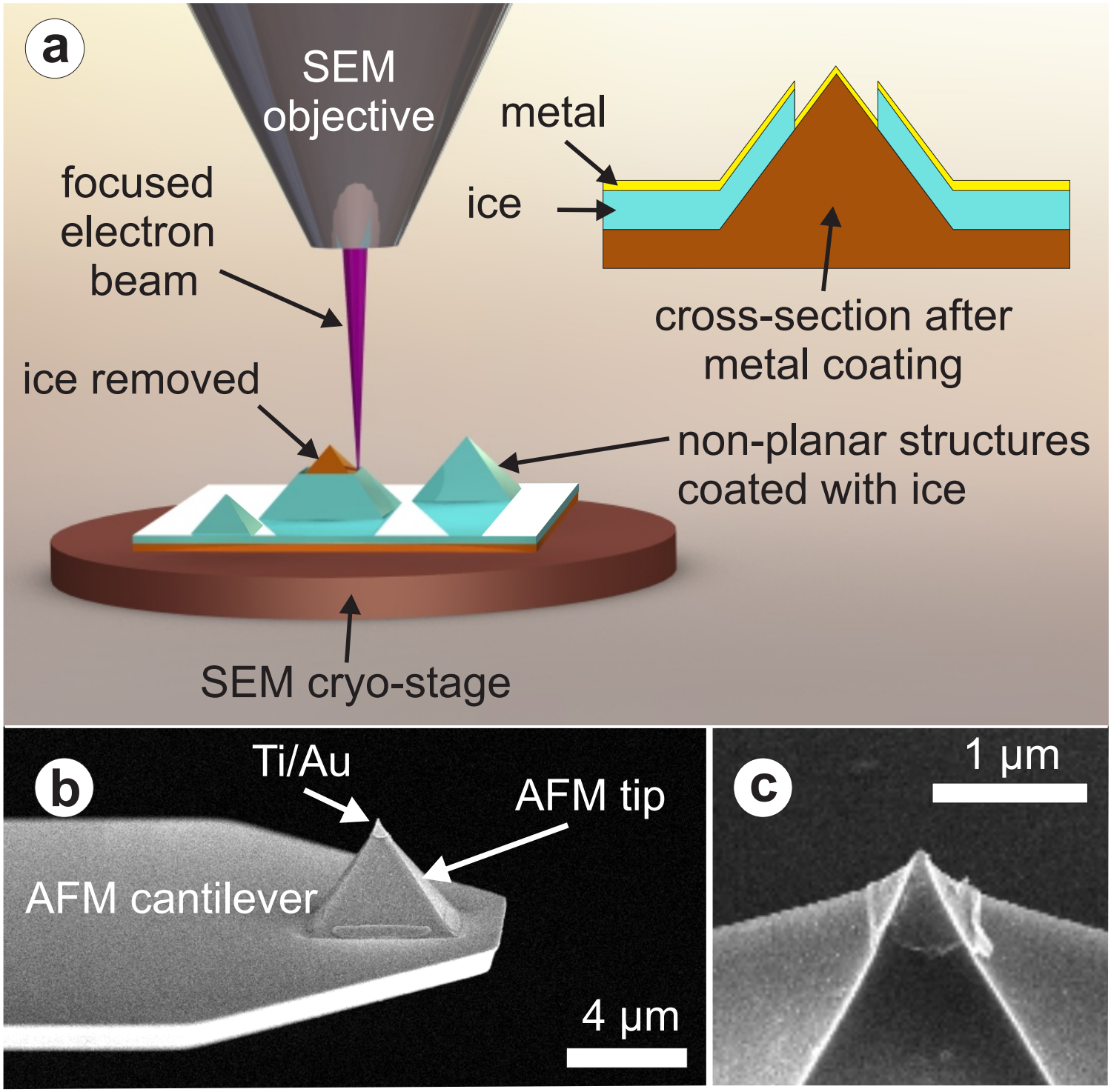

Figure 1. To be published in color.

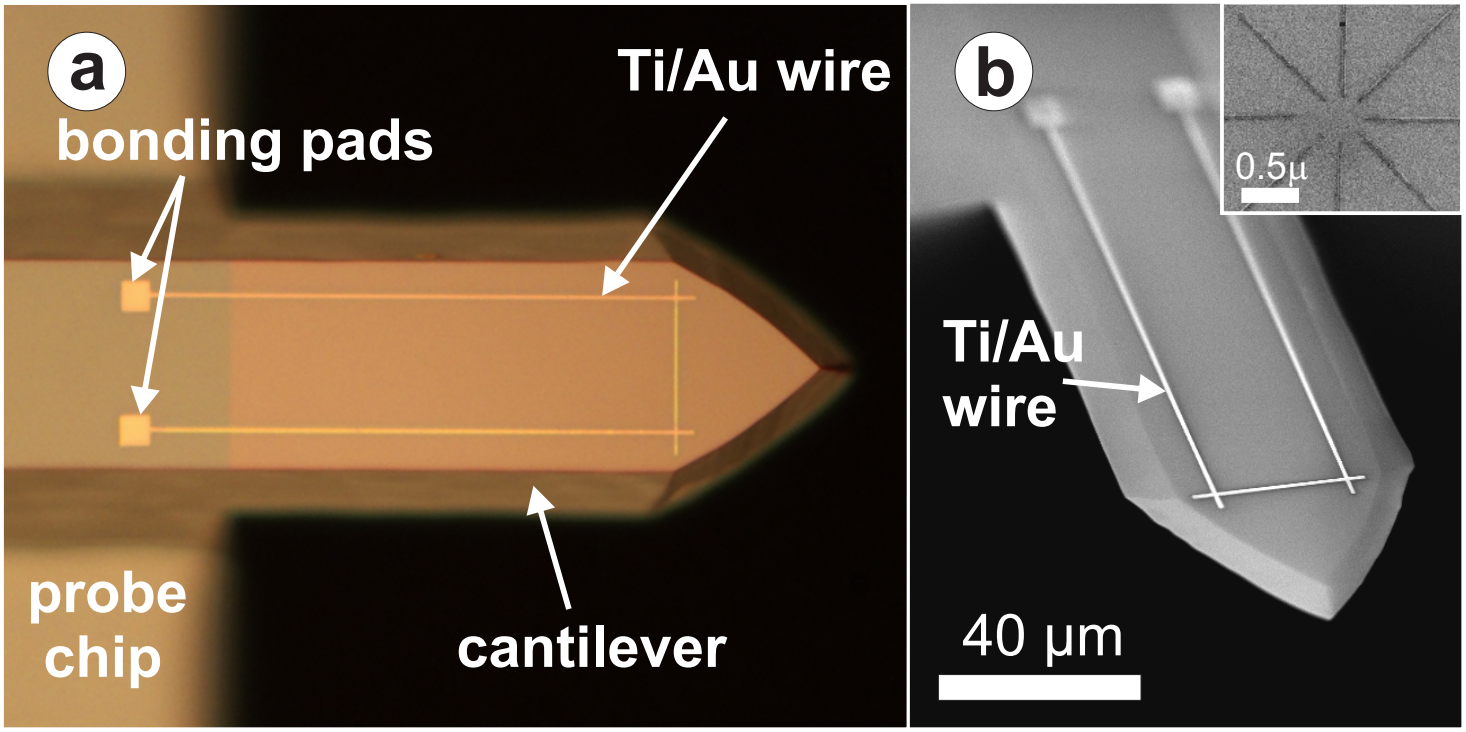

Figure 2. To be published in color.

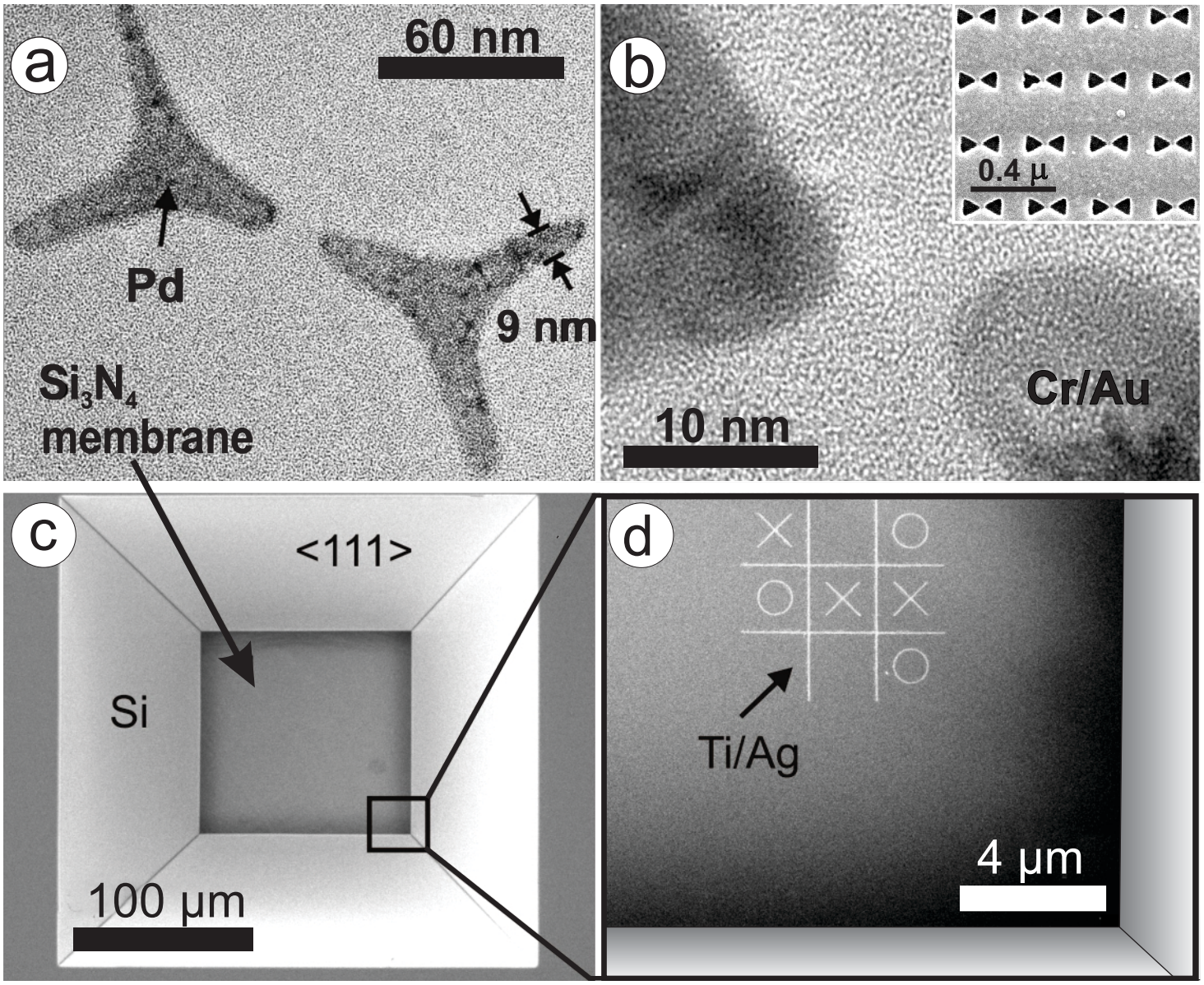

Figure 3. No color needed.

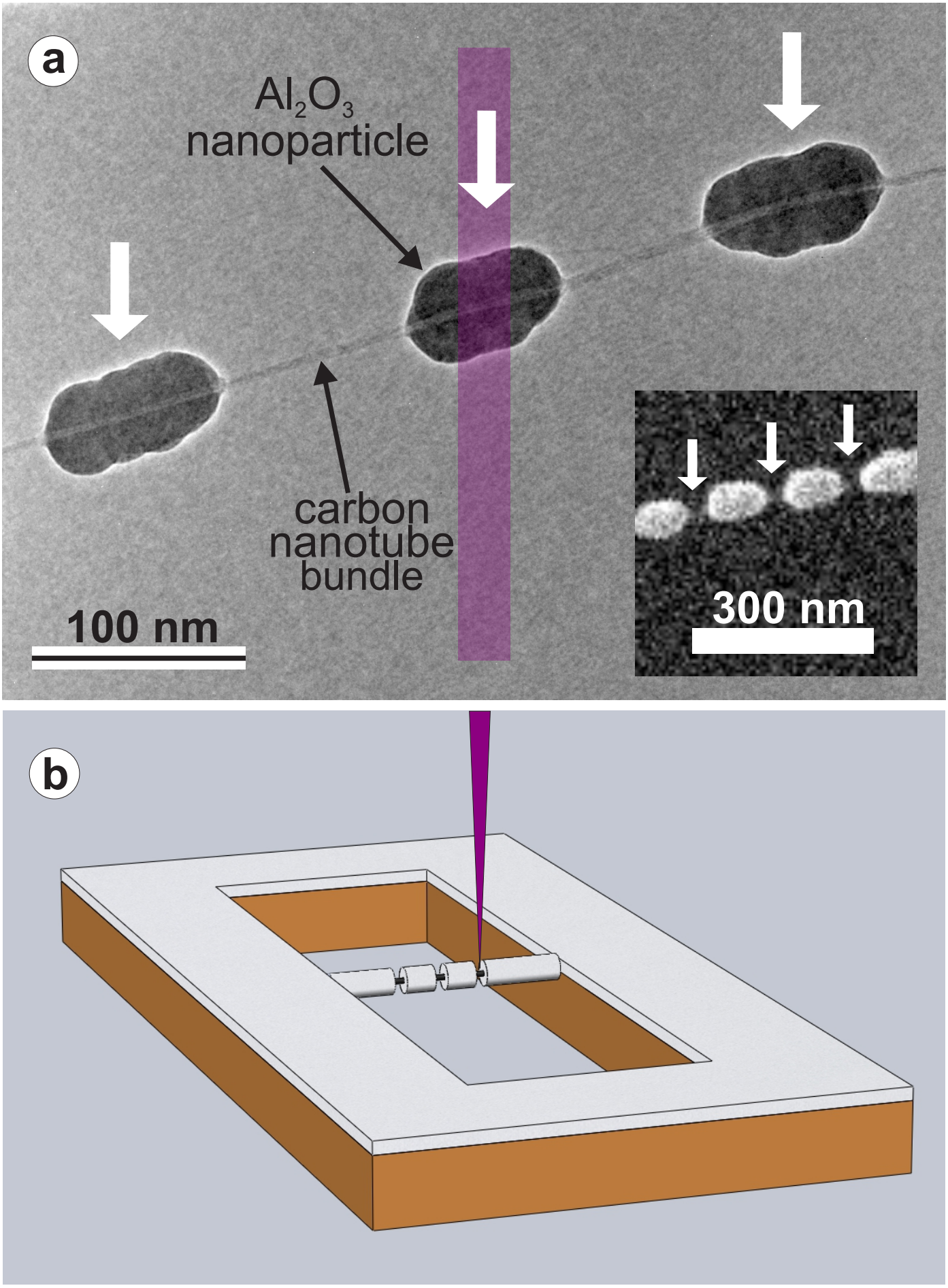

Figure 4. To be published in color.

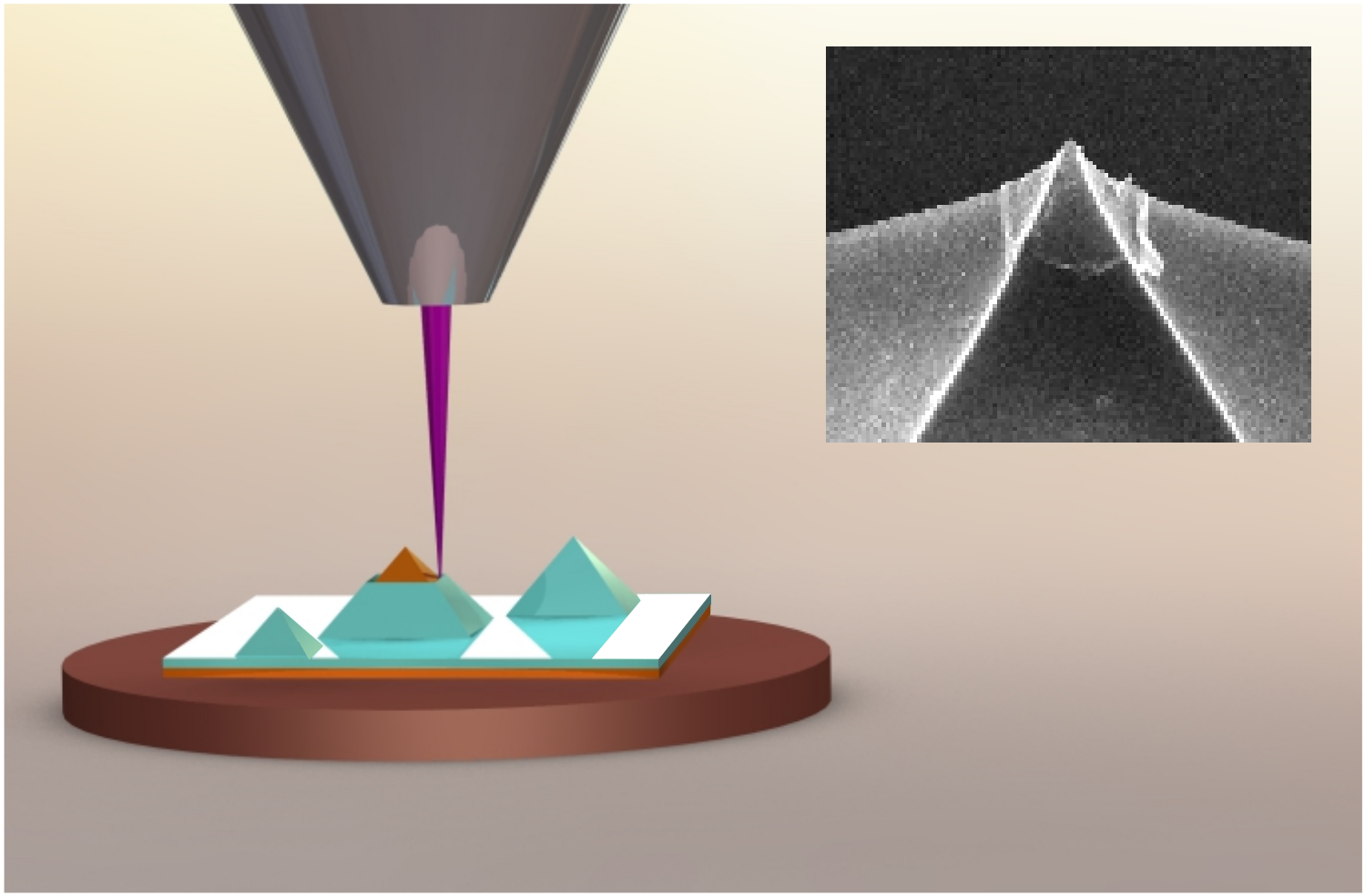

Table of Contents Figure. To be published in color.